Journal of Medicinal Chemistry

Article

pubs.acs.org/jmc

Discovery of Cell-Permeable *O*-GlcNAc Transferase Inhibitors via Tethering in Situ Click Chemistry

Yue Wang,[*,†,‡] Jingjing Zhu,[‡] and Lianwen Zhang[§]

[†]School of Chemistry and Chemical Engineering, University of Chinese Academy of Sciences, Beijing 100049, China

[‡]State Key Laboratory of Natural and Biomimetic Drugs, Peking University, Beijing 100191, China

[§]College of Pharmacy, State Key Laboratory of Medicinal Chemical Biology and Tianjin Key Laboratory of Molecular Drug Research, Nankai University, Tianjin 300071, China

Supporting Information

ABSTRACT: *O*-GlcNAc transferase (OGT) is a key enzyme involved in dynamic *O*-GlcNAcylation of nuclear and cytoplasmic proteins similar to phosphorylation. Discovery of cell-permeable OGT inhibitors is significant to clarify the function and regulatory mechanism of *O*-GlcNAcylation. This will establish the foundation for the development of therapeutic drugs for relevant diseases. Here, we report two cell-permeable OGT inhibitors (APNT and APBT), developed from low-activity precursors (IC_{50} > 1 mM) via "tethering in situ click chemistry (TISCC)". Both of them were able to inhibit *O*-GlcNAcylation in cells without significant effects on cell viability. Unusual noncompetitive inhibition of OGT was helpful to discover novel inhibitors and explore the regulatory mechanism of OGT. The development of these molecules validates that TISCC can be utilized to discover novel lead compounds from components that exhibited very weak binding to the target.

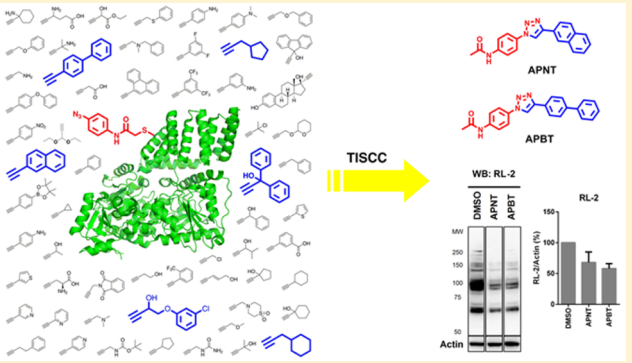

INTRODUCTION

O-GlcNAc transferase (OGT), an essential mammalian enzyme, catalyzes the transfer of *N*-acetylglucosamine from UDP-*N*-acetylglucosamine (UDP-GlcNAc) to hydroxyl groups of serines and threonines (Ser/Thr) in nuclear, cytoplasmic, and mitochondrial proteins,[1,2] such as numerous transcription factors,[3] tumor suppressors, kinases,[4] phosphatases,[5] and histone-modifying proteins.[6] This kind of protein post-translational modification is involved in the regulation of many cellular signaling pathways and closely associated with the occurrence and development of numerous critical illnesses including insulin resistance,[7] diabetic complications,[8] cancer,[9] cardiovascular disease,[10] and Alzheimer's disease.[11] Due to the importance of OGT, various small molecules have been reported to inhibit OGT activity in cells,[12] including alloxan (a uracil mimic),[13] BADGP (a *N*-acetylgalactosamine derivative),[14] Ac4-5SGlcNAc (a metabolic precursor),[15] benzoxazolinone (BZX) derivative (a neutral diphosphate mimic),[16] and OSMI-1 (a quinolinone-6-sulfonamide derivative).[17] However, most of these compounds were not shown to inhibit OGT effectively or selectively. Alloxan also inhibited *O*-GlcNAcase (OGA), which removed *O*-GlcNAc from proteins.[18] BADGP induced abnormal *O*-glycosylation of mucins.[19] Ac4-5SGlcNAc affected several types of cell surface glycans containing mucin-type *O*-glycans.[17] BZX was an irreversible inhibitor of OGT, which was proven too reactive to employ as a selective OGT inhibitor in cells,[16] and OSMI-1 decreased cell viability by about 50% after treatment.[17] All of these were used at millimolar/micromolar concentrations in cells. Therefore, development of OGT inhibitors with novel scaffolds is extremely urgent.

Target-guided synthesis (TGS) is a promising methodology in drug discovery, which can be divided into dynamic combinatorial chemistry and kinetically controlled TGS. Tethering and in situ click chemistry are representative strategies, respectively. The former is a capture method based on thiol−disulfide exchange, where a free thiol on the protein surface can react with a disulfide-containing small fragment to form a disulfide;[20,21] the latter utilizes an irreversible click reaction to combine two reactive building blocks into a potential inhibitory compound.[22−24] Combining the advantages of both approaches, the more general strategy named "tethering in situ click chemistry (TISCC)" is employed herein to discover OGT inhibitors.

RESULTS

In our strategy, one kind of building block is designed with dual reactive groups X (ICH_2CO) and A (N_3) and the other one contains the reactive group Y (C≡CH). First, the target protein is incubated with the former building blocks and therefore tethered with reactive group A (N_3) at several sites.

Received: August 26, 2016

DOI: 10.1021/acs.jmedchem.6b01237
J. Med. Chem. XXXX, XXX, XXX−XXX

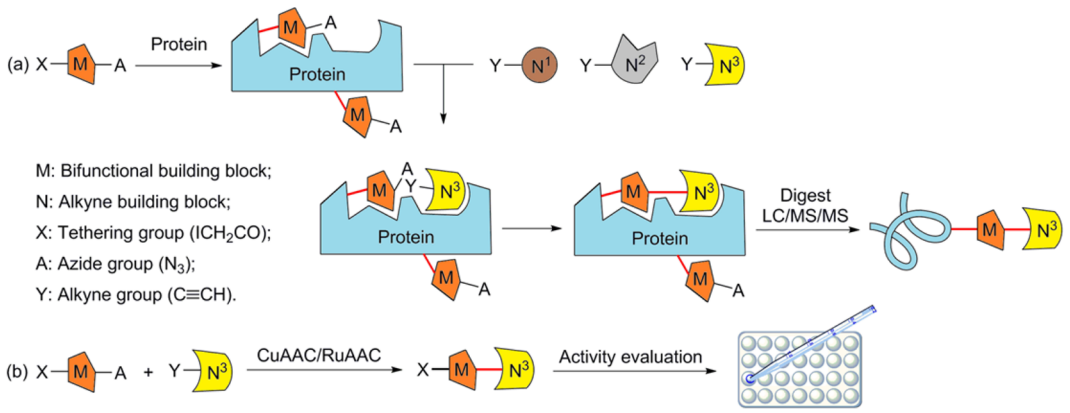

Figure 1. Tethering in situ click chemistry (TISCC): (a) screening of building blocks to discover the new candidate; (b) synthesis of the new candidate for activity evaluation.

Second, the latter building blocks are added to the mixture without separation and then classical in situ click chemistry is performed at proper sites. Finally, the protein is separated from small molecules with SDS−PAGE, digested with trypsin, and then determined with LC/MS/MS to find the modified peptide. The structure of the new candidate can be deduced from the exact mass of modification (Figure 1a). After that, the new candidate was synthesized by copper-/ruthenium-catalyzed azide−alkyne cycloaddition (CuAAC/RuAAC) for activity evaluation (Figure 1b). Compared with tethering and classical in situ click chemistry, our strategy employs more general building blocks and detects the protein fragments instead of the entire protein or biligand compound itself. Therefore, several binding pockets can be screened at the same time.

Iodoacetamide is an alkylating agent used for peptide mapping purposes.[25] It covalently binds with the thiol group of cysteine to prevent the protein from forming disulfide bonds.[26,27] Iodoacetamide inhibits all cysteine peptidases and most of thiol-dependent enzymes irreversibly via nonselective alkylation of the catalytic cysteine residue. Therefore, iodoacetamide was selected as the reactive group X to tether the target protein in our strategy. To maintain proper molecular rigidity, phenyl was used to link the reactive groups X (ICH_2CO) and A (N_3). *p*-Azidoiodoacetanilide (**1**) was chosen to be the difunctional building block.[28]

At first, OGT (10 μM) in Tris-HCl buffer solution containing DTT (1 mM) was incubated with **1** (4 mM) at 37 °C for 2 h. After that, Laemmli sample buffer containing 50 mM DTT was added to quench the reaction. OGT was separated from other reagents with SDS−PAGE, digested with trypsin, and then determined with LC/MS/MS. The results showed most of the cysteine residues in OGT (1−1046 aa) were tethered including Cys44, Cys68, Cys199, Cys267, Cys297, Cys315, Cys323, Cys417, Cys531, Cys590, Cys620, Cys758, Cys845, Cys921, Cys927, Cys962, Cys965 (Figure S1 in Supporting Information). Especially, Cys921 and Cys927, located near the substrate binding site, were tethered with azido groups, and this result encouraged us to perform in situ click chemistry sequentially.

Sixty-one alkyne building blocks were collected including alcohol, ether, acid, amine, steroid, and aromatic compounds and divided into 16 groups (Table S1). Each group was composed of 3−4 components. All the compounds in the same group had an identical functional group as far as possible. For example, every building block in the second group possessed an amino group. According to the native cysteine, the exact mass increases for the expected triazole products were different enough to be distinguished by MS. It seemed to be inefficient to screen 3−4 building blocks for one assay, but nonetheless, it was attractive to screen 17 cysteine residues of OGT at the same time. On the basis of the foregoing procedure, alkynes were added to the tethering reaction mixtures without separation and the resulting mixtures were kept at 37 °C for another 6 h (Figure S2) before being quenched. Fourteen different modifications were found on only four cysteine residues including Cys590, Cys758, Cys921, and Cys927 (Chart 1).

Chart 1. Structures of Building Blocks and Relevant Triazoles[a]

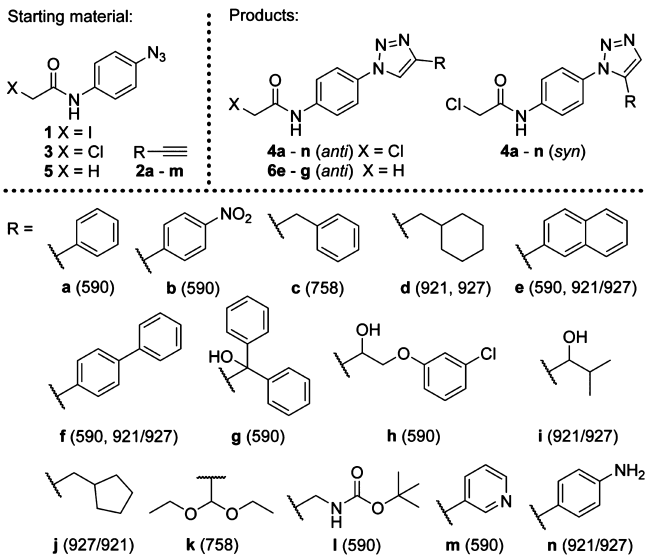

[a]Modification sites of OGT found with LC/MS/MS shown in paratheses.

To examine the efficiency of TISCC, *anti*- and *syn*-triazoles (**4a−n**) were synthesized by CuAAC and RuAAC, respectively.[29,30] Instead of iodine (**1**), chloride (**3**) was employed to reduce off-target effects. All the compounds were produced successfully except ***syn*-4l,m,n** and ***anti*-4n**, probably because the nitrogen atom present in alkynes **2l**, **2m**, and **2n** bound to the ruthenium/copper atom suppressing its catalytic activity.[31]

DOI: 10.1021/acs.jmedchem.6b01237
J. Med. Chem. XXXX, XXX, XXX−XXX

All the compounds were then evaluated for OGT inhibition activity with HPLC assay that monitored the transfer of GlcNAc to an OGT acceptor peptide (CKII). Eight of these 22 compounds inhibited OGT > 40% at 100 μM, while the precursors **1** and **3** showed no significant inhibitory effect at this concentration (Figure S3). To identify the cysteine sites that reacted with these eight candidates, tryptic digests of OGTs were analyzed following treatment with the candidates, respectively. The modifications of cysteines were determined at the Cys590 or adjacent Cys531/Cys620 except ***anti*-4e** and **-f**. Therefore, we focused on ***anti*-4e**, **-f**, and **-g** for further investigation. An inactivation time course showed that OGT inhibition of ***anti*-4g** was time-dependent; however, OGT preincubated with ***anti*-4e** or **-f** kept most of the enzyme activity during the period of measurement (Figure S4). IC_{50} values were determined for the positive control (BZX), the precursors (**1**, **2e**−**g**, and **3**) and candidates (***anti*-4e**, **-f**, and **-g**) (Table 1, entries 1−9 and Figure S5). IC_{50} values of three candidates were dramatically lower than those of the precursors (**1**, **2e**−**g**, and **3**).

Table 1. IC_{50} Values of Several Compounds

entry	compd	IC_{50} (μM)
1	BZX	11.9 ± 1.1
2	**1**	865 ± 43
3	**2e**	>4000 (88 ± 1%)[a]
4	**2f**	>1000 (79 ± 2%)[b]
5	**2g**	1964 ± 13
6	**3**	3967 ± 209
7	***anti*-4e**	71.7 ± 1.0
8	***anti*-4f**	91.2 ± 1.9
9	***anti*-4g**	89.3 ± 1.8
10	**5**	>4000 (64% ± 1%)[a]
11	***anti*-6e** (APNT)	66.7 ± 0.8
12	***anti*-6f** (APBT)	139 ± 14
13	***anti*-6g**	1001 ± 8

[a]Enzyme activity in the presence of 4000 μM inhibitor. [b]Enzyme activity in the presence of 1000 μM inhibitor.

We next examined the ability of three candidates (***anti*-4e**, **-f**, and **-g**) to inhibit global *O*-GlcNAcylation in COS-7 cells. Unfortunately, all of the three candidates showed strong cytotoxicity probably arising from the chloroacetamide group. Therefore, corresponding acetamide derivatives (***anti*-6e**, **-f**, and **-g**) were synthesized from *p*-azidoacetanilide (**5**) via similar procedures. OGT inhibition assay showed that ***anti*-6e** (APNT) and ***anti*-6f** (APBT) kept intrinsic activities; nevertheless, ***anti*-6g** presented less inhibition activity (Table 1, entries 11−13, and Figure S6). The removal of the activated leaving group (Cl) in ***anti*-6g** and resulting loss of inhibition activity confirmed that ***anti*-4g** was an irreversible inhibitor. With the commercially available UDP-Glo glycosyltransferase assay, the mode of inhibition was determined for APNT and APBT, both of which were found to be noncompetitive with respect to UDP-GlcNAc (K_m = 10.3 ± 0.3 μM, $K_{i,APNT}$ = 28.6 ± 0.5 μM, $K_{i,APBT}$ = 92.0 ± 3.0 μM) or CKII peptide (K_m = 230 ± 16 μM, $K_{i,APNT}$ = 59.8 ± 2.8 μM, $K_{i,APBT}$ = 310 ± 17 μM) (Figure 2). In addition, we tested the effect of APNT and APBT on ppGalNAcT2.[32] Neither of them inhibited ppGalNAcT2 remarkably ($IC_{50,APNT}$ = 696 ± 69 μM, $IC_{50,APBT}$ = 430 ± 35 μM) (Figure S7).

COS-7 cells were treated for 4 h in glucose starvation medium with varying concentrations of APNT or APBT ranging from 12.5 to 100 μM. After that, glucosamine (2 mM) and PUGNAc (100 μM) were added to the cells and incubated for another 3 h. Finally, cell lysates were detected with the *O*-GlcNAc antibody (RL-2). APNT and APBT reduced global *O*-GlcNAcylation (Figures 3 and S8) in a dose-dependent manner (Figure S9) with the maximal effect being accomplished at 25 μM. As a result of the limited aqueous solubility of APNT and APBT, higher concentrations of APNT or APBT did not decrease *O*-GlcNAc levels further. Although APNT and APBT showed weaker inhibition of OGT than BZX in vitro, they were comparable with BZX in vivo. In addition to the reduction of global *O*-GlcNAcylation in cells, the effects of APNT and APBT on specific cellular markers of OGT inhibition were investigated. It was found that APNT and APBT, like BZX, reduced cellular OGA, which decreased when cellular *O*-GlcNAcylation was blocked. However, OGT levels remain unchanged (Figure 3).[17] Therefore, we concluded that APNT and APBT inhibited OGT activity in cells.

We used lectins to probe cell surface glycans following the treatment of cells with APNT and APBT. Eight commercially available biotinylated lectins (ConA, LCA, Jacalin, PHA-E, ECL, GSL-I, PNA, and DBA), which recognize different features of *N*- and *O*-glycans, were employed to probe the glycan composition of COS-7 cells treated with 100 μM APNT or APBT for 7 h. For positive control (BZX), APNT and APBT, all of the ConA, PNA, and DBA levels were kept between 80% and 120% compared with negative control (DMSO). For BZX, GSL-I level increased by over 20% while PHA-E level decreased by over 20%. For APNT and APBT, LCA, Jacalin, ECL and GSL-I levels increased by over 20%. Especially, Jacalin and ECL levels changed dramatically (136−173%), which are relative to Galβ3GalNAc and Galβ4GlcNAc, respectively. This phenomenon implies that some kind of galactosyltransferase is likely to be regulated by *O*-GlcNAcylation (Figures 4 and S10).

Furthermore, we found no obvious effects on cell viability following the treatment of cells with APNT and APBT (Figure S11).

DISCUSSION AND CONCLUSIONS

In summary, we developed cell-permeable OGT inhibitors (APNT and APBT) via TISCC and follow-up chemistry. Traditional in situ click chemistry always utilized building blocks with a high affinity for the target ($IC_{50} \leq 6.4$ μM). When the IC_{50} of the precursor had a micromolar concentration, the newly produced inhibitor expressed (5−700)-fold increase in the inhibitory activity.[33−35] Click chemistry was also employed to discover fucosyltransferase inhibitors from GDP-alkyne (K_i = 47 μM), following in situ screening without product isolation.[36] However, the diphosphate bridge, which contributed considerably to binding affinity, prevented the resultant inhibitor from entering the cells. Here, APNT (IC_{50} = 66.7 ± 0.8 μM) was composed of two neutral building blocks **2e** and **5**, which exhibited very weak binding to OGT (IC_{50} > 4000 μM) (Table 1, entries 3, 10, and 11). The newly produced inhibitor showed more than 60-fold increase in the inhibitory activity, the effect of which was comparable with that of BZX in vivo. Therefore, TISCC could be used to screen precursors with poor activity, the IC_{50} of which was around several millimolar.

Different from most OGT inhibitors, APNT and APBT were noncompetitive with respect to UDP-GlcNAc or CKII peptide.

DOI: 10.1021/acs.jmedchem.6b01237
J. Med. Chem. XXXX, XXX, XXX−XXX

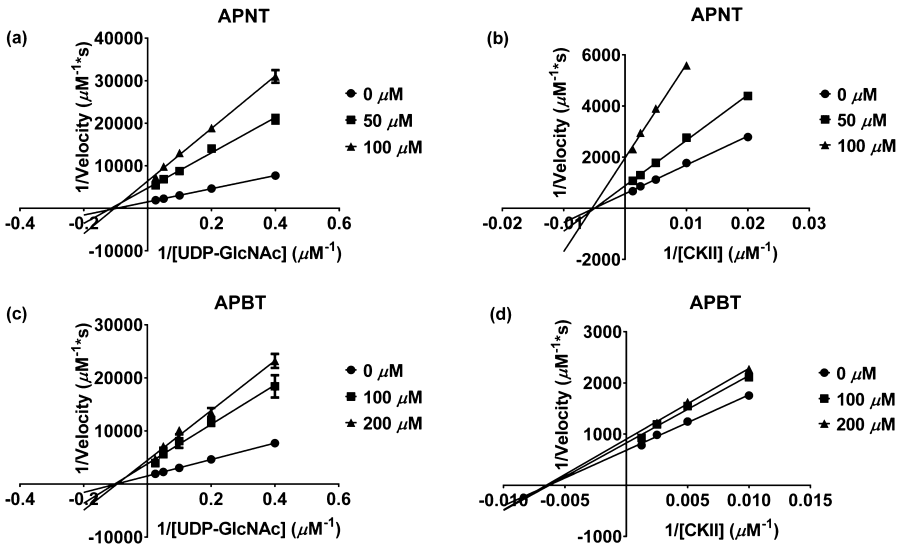

Figure 2. Noncompetitive inhibition of OGT by APNT and APBT with respect to UDP-GlcNAc or CKII peptide. (a, c) Double reciprocal plot showed noncompetitive inhibition of OGT by APNT/APBT at saturating CKII concentrations. Reactions were performed in the presence of APNT/APBT at saturating peptide concentrations while varying UDP-GlcNAc levels (conditions: 25 nM OGT, 3 mM CKII, UDP-GlcNAc varied from 2.5 to 40 μM and APNT/APBT at the indicated, fixed concentrations; 1 h incubation at room temperature). (b, d) Double reciprocal plot showed noncompetitive inhibition of OGT by APNT/APBT at saturating UDP-GlcNAc concentrations. Reactions were performed in the presence of APNT/APBT at saturating UDP-GlcNAc concentrations while varying CKII concentrations (conditions: 50 nM OGT, 1 mM UDP-GlcNAc, CKII varied from 50 to 800 μM and APNT/APBT at the indicated, fixed concentrations; 1 h incubation at room temperature). Each point was determined in triplicate experiments.

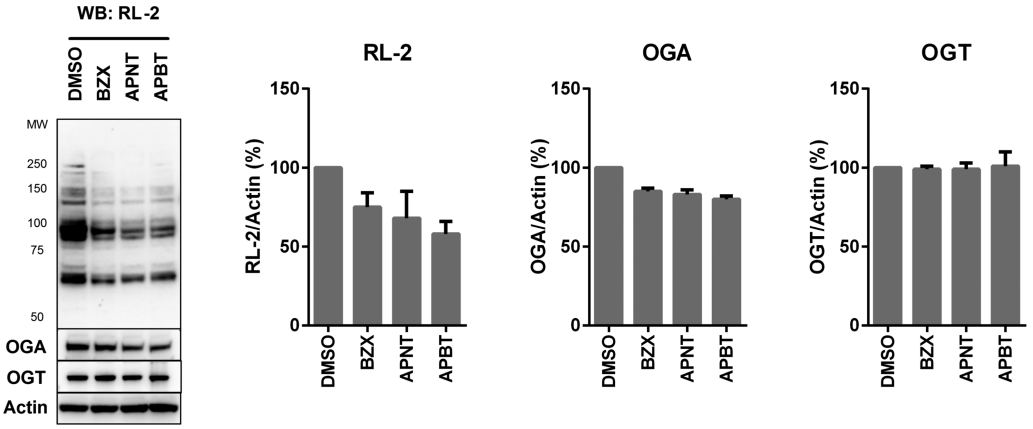

Figure 3. Inhibition of OGT by APNT and APBT in cells. Lysates from COS-7 cells, untreated or treated with inhibitors at 100 μM, were detected for global *O*-GlcNAc, OGA, and OGT levels. Accompanied with the reduction of global *O*-GlcNAc levels, APNT and APBT decreased OGA levels without affecting OGT levels.

According to the results of TISCC, APNT was likely to bind to the pocket around Cys590. Docking APNT with OGT-UDP-CKII complex (PDB code 3PE4), we found that APNT bound the cleft between the TPR domain and the N-terminal domain of the catalytic region (Figure S12). This information can be used to design novel OGT inhibitors and understand regulatory mechanisms of OGT. For further investigation, improvement of aqueous solubility of APNT and APBT is urgent and the second round of in situ click chemistry will be performed on the basis of APNT and APBT.

EXPERIMENTAL SECTION

Tethering in Situ Click Chemistry. Reaction mixtures containing 10 μM OGT, 4 mM *p*-azidoiodoacetanilide (**1**), and buffer (150 mM NaCl, 1 mM DTT, 25 mM Tris-HCl, pH = 7.4) were incubated at 37 °C for 2 h. Without separation, alkynes were added at the final concentration of 1 mM for each building block, and the resulting mixtures were kept at 37 °C for another 6 h. Then reactions were quenched by adding Laemmli sample buffer (Biorad) containing 50 mM DTT and boiling samples at 96 °C for 10 min. SDS−PAGE was performed using precast Any kD Mini-PROTEAN TGX Gel (Biorad), followed by staining with GelCode Blue stain reagent (Thermo Scientific) for 1 h and destaining with distilled water for 1 h.

In-Gel Trypsin Digestion. Each OGT lane was cut into 10 pieces and reduced with 25 mM DTT, but there was no need to alkylate with iodoacetamide. Then, in-gel digestion was carried out with sequencing grade modified trypsin (Promega) in 50 mM ammonium bicarbonate at 37 °C overnight. Tryptic peptides were extracted twice with 1% trifluoroacetic acid in 50% acetonitrile aqueous solution for 30 min. The extractions were then centrifuged in a SpeedVac to reduce the volume.

LC/MS/MS Analysis. The digestion products were separated by an 85 min gradient elution at a flow rate of 0.250 μL/min with an Ultimate 3000 HPLC system (Thermo Scientific), which was directly interfaced with a Orbitrap Q Exactive mass spectrometer (Thermo

DOI: 10.1021/acs.jmedchem.6b01237
J. Med. Chem. XXXX, XXX, XXX−XXX

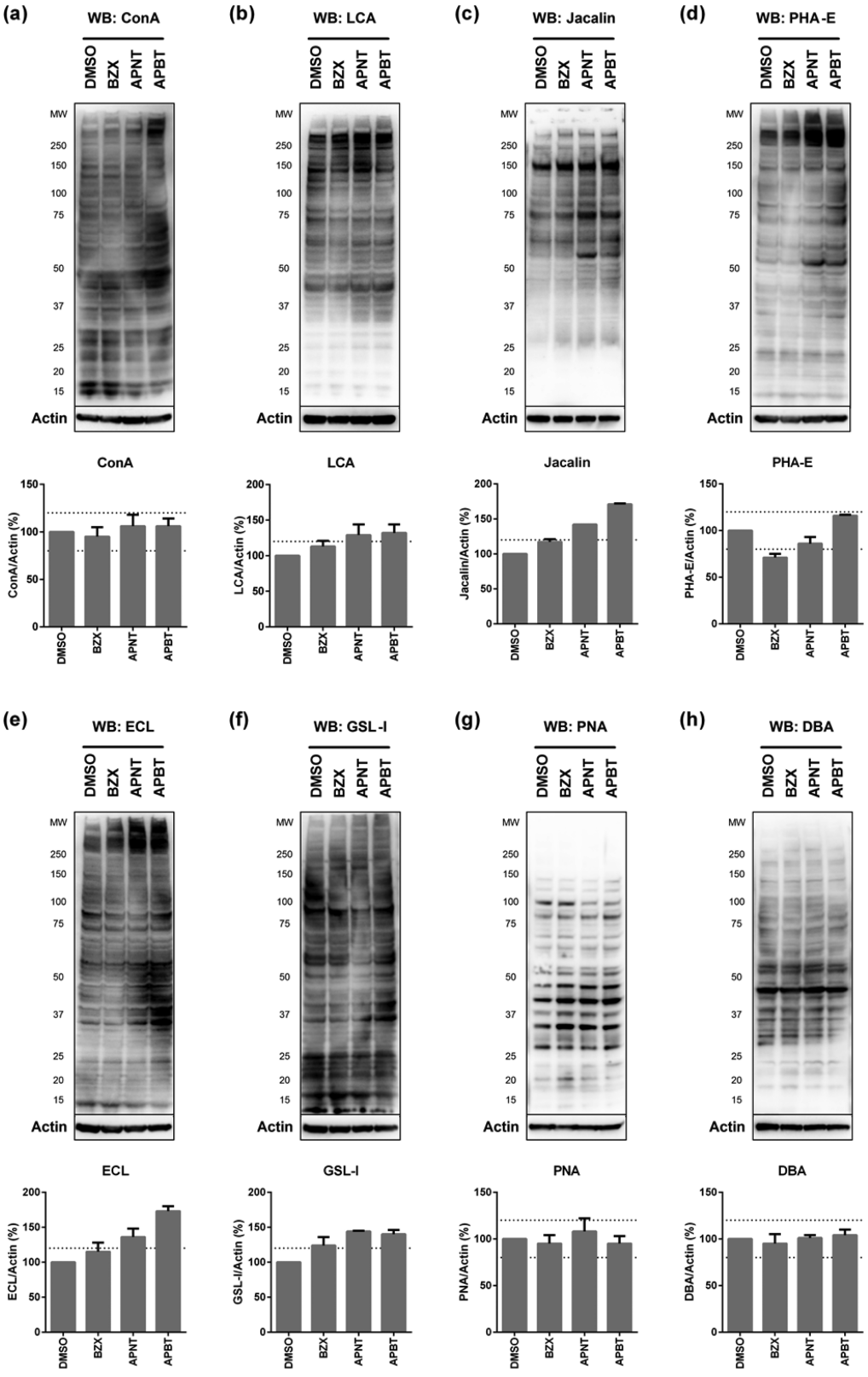

Figure 4. Effect of OGT inhibitors on cell surface glycans. Lysates from COS-7 cells, untreated or treated with inhibitors at 100 μM, were probed with lectins. For APNT and APBT, LCA, Jacalin, ECL, and GSL-I levels increased by over 20% while ConA, PHA-E, PNA and DBA levels were kept between 80% and 120% compared with negative control (DMSO). According to data sheet of Vector Laboratories, preferred sugar specificity of each lectin appears to be as follows: concanavalin A (Con A) and *Lens culinaris* (LCA) recognize αMan and αGlc; Jacalin recognizes Galβ3GalNAc; *Phaseolus vulgaris* erythroagglutinin (PHA-E) recognizes Galβ4GlcNAcβ2Manα6(GlcNAcβ4)(GlcNAcβ4Manα3)Manβ4; *Erythrina cristagalli* (ECL) recognizes Galβ4GlcNAc; *Griffonia* (*Bandeiraea*) *simplicifolia* I (GSL-I) recognizes αGal and αGalNAc; peanut agglutinin (PNA) recognizes Galβ3GalNAc; *Dolichos biflorus* (DBA) recognizes αGalNAc.

DOI: 10.1021/acs.jmedchem.6b01237
J. Med. Chem. XXXX, XXX, XXX−XXX

Scientific). The analytical column was a homemade fused silica capillary column (75 μm × 150 mm; Upchurch) packed with C-18 resin (300 Å, 5 μm; Varian). Mobile phase A consisted of 0.1% formic acid in H_2O and mobile phase B consisted of 0.1% formic acid in MeCN. The Q Exactive mass spectrometer was operated in the data-dependent acquisition mode using Xcalibur 2.1.2 software, and there was a single full-scan mass spectrum in the orbitrap (400−1 800 m/z, 60 000 resolution) followed by 10 data-dependent MS/MS scans at 27% normalized collision energy (HCD).

The MS/MS spectra from each LC/MS/MS run were searched against the human.fasta from UniProt (release date of March 19, 2014; 68 406 entries) using an in-house Proteome Discoverer (version PD1.4, Thermo Scientific). The search criteria were as follows: full tryptic specificity was required; one missed cleavage was allowed; the oxidation (Met) and expected modifications (Cys) (for example, the increase of exact mass is 174.0542 or 148.0637 according to the native cysteine) were set as the variable modifications; precursor ion mass tolerances were set at 10 ppm for all MS data acquired in an orbitrap mass analyzer; and the fragment ion mass tolerance was set at 20 mmu for all MS^2 spectra acquired.

OGT Activity Assay with HPLC. Reaction mixtures containing 200 μM CKII peptide (KKKYPGGSTPVSSANM M), 1 mM UDP-GlcNAc, 100 nM ncOGT, 12.5 mM $MgCl_2$, buffer (150 mM NaCl, 1 mM EDTA, 2.5 mM tris(hydroxypropyl)phosphine, 20 mM Tris-HCl, pH 7.4), and inhibitor (if necessary) were incubated at 37 °C for 30 min (for determination of OGT stability) or 60 min (for inhibitor screening and IC_{50} determination). After being quenched by adding an equal volume of methanol, the reaction mixtures were centrifuged at 12 000g for 30 min. The supernatants (40 μL) were loaded onto an Agilent 1260 Infinity HPLC system to quantify the yield based on the integrated areas of glycopeptide product and peptide substrate. The reverse-phase chromatographic column was a Zorbax SB-C18 StableBond analytical column (4.6 mm × 250 mm, 5 μm; Agilent), preceded by a Zorbax SB-C18 analytical guard column (4.6 mm × 12.5 mm, 5 μm; Agilent). Mobile phase A consisted of 0.1% TFA in H_2O, and mobile phase B consisted of 0.1% TFA in MeCN. The components were eluted using a gradient (flow rate at 1 mL/min; at 0 min elution solvent mixture A/B = 90/10; at 20 min elution solvent mixture A/B = 70/30; wavelength = 214 nm). Each reaction was repeated twice or three times.

Western Blot of Inhibitor-Treated COS-7 Cells. COS-7 cells were maintained in DMEM (Hyclone) supplemented with 10% fetal bovine serum (Gibco), 100 U/mL penicillin, and 100 μg/mL streptomycin (MP). Old growth medium was removed when cells were grown to 70% confluence. After being rinsed twice with PBS, cells were grown in glucose starvation medium (DMEM-no glucose; Caisson Labs) supplemented with 1% fetal bovine serum, 50 U/mL penicillin, and 50 μg/mL streptomycin) in the absence (control) and presence of inhibitor (100 μM) for 4 h. Glucosamine (2 mM, Sigma) and PUGNAc (100 μM, Santa Cruz Biotechnology) were added to the cells and then incubated for another 3 h. Cell lysates were prepared in RIPA lysis buffer (Beyotime) supplemented with protease inhibitor cocktail (Pierce). Lysates were centrifuged at 16 000g for 15 min at 4 °C and analyzed by SDS−PAGE (4−12%, Invitrogen). Proteins were transferred to a PVDF membrane (Millipore), and *O*-GlcNAcylation was detected with anti-*O*-GlcNAc antibody (RL-2, Abcam, used at 1:1 000) and a secondary anti-mouse IgG-HRP antibody (Jackson ImmunoResearch, used at 1:10 000). OGT, OGA, and actin were detected with relevant antibodies (Sigma/MDL Biotech, used at 1:2 000) and a secondary anti-rabbit lgG-HRP antibody (Jackson ImmunoResearch, used at 1:10 000). Cell surface glycans was probed with biotinylated lectins (Vector Laboratories, used at 1:2 00) and HRP-conjugated streptavidin (CST, used at 1:2 000).

General Procedures for Chemical Synthesis. All chemicals were purchased as reagent grade and used without further purification. Reactions were monitored by analytical thin-layer chromatography on silica gel 60 F254 precoated on aluminum plates (E. Merck). Spots were detected under UV (254 nm) and/or by staining with acidic ceric ammonium molybdate. Solvents were evaporated under reduced pressure below 40 °C (bath). Column chromatography was performed on silica gel (200−300 mesh, Tsingdao Haiyang). ^1H NMR and ^{13}C NMR spectra were recorded on a Bruker AVANCE III 400 spectrometer at 25 °C. Chemical shifts (in ppm) of ^1H NMR were calibrated with tetramethylsilane (δ = 0 ppm) or solvent residual peak (δ = 2.50 ppm for CD_3SOCD_2H). Chemical shifts (in ppm) of ^{13}C NMR were calibrated with solvent peak (δ = 77.16 ppm for $CDCl_3$ and δ = 39.52 ppm for CD_3SOCD_3). Mass spectra were recorded using a Waters Xevo G2 Q-TOF spectrometer (ESI) or a Thermo Finnigan TRACE 2000/Waters GCT Premier (EI). Elemental analysis was performed with a Vario EL III analyzer. Percentages of purity were determined with HPLC for the compounds, the purity of which was not verified with elemental analysis. All the compounds possessed the purity of at least 95%.

***p*-Azidochloroacetanilide (3) and *p*-Azidoacetanilide (5).** Following a literature procedure,[37] the mixture of *p*-iodoaniline (10.95 g, 50.0 mmol), sodium azide (6.50 g, 100 mmol, 2 equiv), sodium ascorbate (0.55 g, 2.78 mmol, 5.6%), and DMSO/H_2O (V/V = 5/1, 110 mL) was placed in a two-neck round-bottom flask. Argon was passed through the solution for 5 min. CuI (0.95 g, 5.0 mmol, 10%) and *N*,*N*′-dimethylethylenediamine (0.85 mL, 7.9 mmol, 16%) were added to the reaction mixture under argon atmosphere. The reaction was stirred at room temperature for 1 h, and TLC analysis showed complete consumption of the starting material. The reaction mixture was subsequently diluted with water (150 mL) and extracted with ethyl acetate (3 × 150 mL). The organic layers were combined, washed with brine (3 × 50 mL), dried over Na_2SO_4, filtered, and evaporated under reduced pressure. The resulting residue was purified by flash chromatography (ethyl acetate/petrol ether, V/V = 1/4) to yield *p*-azidoaniline (7) (5.44 g, 40.6 mmol, 81%). ^1H NMR (400 MHz, $CDCl_3$) δ 7.40 (d, J = 8.1 Hz, 2H, phenyl), 6.47 (d, J = 8.2 Hz, 2H, phenyl), 3.67 (s, 2H, NH_2).

Compound 7 (6.57 g, 49.0 mmol), chloroacetic acid (4.63 g, 49.0 mmol, 1.0 equiv), and 1-(3-dimethylaminopropyl)-3-ethylcarbodiimide hydrochloride (18.79 g, 98.0 mmol, 2.0 equiv) were dissolved in dry THF (265 mL). The reaction was stirred at room temperature for 2 h and then evaporated under reduced pressure. The resulting residue was redissolved in ethyl acetate (700 mL), washed successively with 1 M HCl (3 × 300 mL), aq $NaHCO_3$ (3 × 200 mL) and brine (150 mL), dried over Na_2SO_4, filtered, and evaporated under reduced pressure to yield **3** (9.85 g, 46.8 mmol, 95%). ^1H NMR (400 MHz, $CDCl_3$) δ 8.24 (s, 1H, NH), 7.55 (d, J = 8.7 Hz, 2H, phenyl), 7.02 (d, J = 8.7 Hz, 2H, phenyl), 4.20 (s, 2H, $ClCH_2CO$). ^{13}C NMR (101 MHz, $CDCl_3$) δ 163.89 (C═O), 136.97 (C-Ar), 133.75 (C-Ar), 121.78 (CH-phenyl), 119.77 (CH-phenyl), 42.96 ($ClCH_2CO$). HRMS (EI-TOF) m/z: $[M]^+$ calcd for $C_8H_7N_4OCl$ 210.0308; found 210.0309.

Compound **5** was obtained via a similar procedure. ^1H NMR (400 MHz, $CDCl_3$) δ 7.50 (d, J = 8.8 Hz, 2H, phenyl), 7.23 (s, 1H, NH), 6.98 (d, J = 8.8 Hz, 2H, phenyl), 2.18 (s, 3H, CH_3CO). HRMS (ESI-TOF) m/z: $[M + H]^+$ calcd for $C_8H_9N_4O$ 177.0776; found 177.0778.

General Procedure for Copper-Catalyzed Alkyne−Azide Cycloaddition. Compound **3** or **5** (0.500 mmol) and alkyne (0.600 mmol, 1.2 equiv) were stirred together in *t*-butanol/water (V/V = 2/1, 5.0 mL) under argon. To this suspension was added aq copper sulfate (0.50 M, 50 μL, 5.0%) and aq sodium ascorbate (0.10 M, 500 μL, 10%). The reaction was stirred at 50 °C until TLC analysis showed complete consumption of the starting material (**3** or **5**). The precipitate was collected by filtration, washed with aq EDTA (0.1 M, 3 × 5 mL), aq $NaHCO_3$ (5 mL), water (3 × 5 mL), and diethyl ether (2 × 5 mL) successively and then dried overnight in a vacuum desiccator to yield the desired *anti*-triazole (**4** or **6**).

1-(4-Chloroacetamidophenyl)-4-phenyl-1*H*-1,2,3-triazole (*anti*-4a). ^1H NMR (400 MHz, CD_3SOCD_3) δ 10.59 (s, 1H, NH), 9.24 (s, 1H, triazole), 8.00−7.88 (m, 4H, phenyl), 7.83 (d, J = 9.0 Hz, 2H, phenyl), 7.50 (t, J = 7.6 Hz, 2H, phenyl-3′/5′), 7.38 (t, J = 7.4 Hz, 1H, phenyl-4′), 4.31 (s, 2H, $ClCH_2CO$). ^{13}C NMR (101 MHz, CD_3SOCD_3) δ 164.96 (C═O), 147.22 (C-Ar), 138.75 (C-Ar), 132.29 (C-Ar), 130.28 (C-Ar), 128.98 (CH-phenyl-3′/5′), 128.20 (CH-phenyl-4′), 125.32 (CH-phenyl-2′/6′), 120.75 (CH-phenyl), 120.24 (CH-phenyl), 119.47 (CH-triazole), 43.54 ($ClCH_2CO$). ESI-MS ($m/$

DOI: 10.1021/acs.jmedchem.6b01237
J. Med. Chem. XXXX, XXX, XXX−XXX

z, relative intensity): 313 ([M + H]$^+$, 100) , 279 (12), 114(11). Anal. Calcd for $C_{16}H_{13}N_4OCl$: C, 61.45; H, 4.19; N, 17.91. Found: C, 61.29; H, 4.22; N, 17.91.

1-(4-Chloroacetamidophenyl)-4-(4-nitrophenyl)-1*H*-1,2,3-triazole (*anti*-4b). ^{1}H NMR (400 MHz, CD_3SOCD_3) δ 10.60 (s, 1H, NH), 9.50 (s, 1H, triazole), 8.37 (d, J = 8.8 Hz, 2H, phenyl), 8.20 (d, J = 8.7 Hz, 2H, phenyl), 7.92 (d, J = 8.9 Hz, 2H, phenyl), 7.84 (d, J = 8.9 Hz, 2H, phenyl), 4.31 (s, 2H, $ClCH_2CO$). ^{13}C NMR (101 MHz, CD_3SOCD_3) δ 165.00 (C═O), 146.82 (C-Ar), 145.27 (C-Ar), 139.03 (C-Ar), 136.68 (C-Ar), 132.00 (C-Ar), 126.09 (CH-phenyl), 124.48 (CH-phenyl), 121.60 (CH-triazole), 120.92 (CH-phenyl), 120.25 (CH-phenyl), 43.55 ($ClCH_2CO$). ESI-MS (*m*/*z*, relative intensity): 358 ([M + H]$^+$, 100). Anal. Calcd for $C_{16}H_{12}N_5O_3Cl$: C, 53.72; H, 3.38; N, 19.58. Found: C, 53.65; H, 3.44; N, 19.41.

1-(4-Chloroacetamidophenyl)-4-benzyl-1*H*-1,2,3-triazole (*anti*-4c). ^{1}H NMR (400 MHz, CD_3SOCD_3) δ 10.54 (s, 1H, NH), 8.53 (s, 1H, triazole), 7.84 (d, J = 9.0 Hz, 2H, phenyl), 7.77 (d, J = 9.0 Hz, 2H, phenyl), 7.41−7.26 (m, 4H, phenyl-2′/3′/5′/6′), 7.26−7.15 (m, 1H, phenyl-4′), 4.29 (s, 2H, $ClCH_2CO$), 4.08 (s, 2H, $ArCH_2$). ^{13}C NMR (101 MHz, CD_3SOCD_3) δ 164.89 (C═O), 147.06 (C-Ar), 139.28 (C-Ar), 138.47 (C-Ar), 132.39 (C-Ar), 128.52 (CH-phenyl-2′/6′/3′/5′), 128.44 (CH-phenyl-3′/5′/2′/6′), 126.22 (CH-phenyl-4′), 120.60 (CH-triazole), 120.57 (CH-phenyl), 120.15 (CH-phenyl), 43.52 ($ClCH_2CO$), 31.20 ($ArCH_2$). ESI-MS (*m*/*z*, relative intensity): 327 ([M + H]$^+$, 100). Anal. Calcd for $C_{17}H_{15}N_4OCl$: C, 62.48; H, 4.63; N, 17.15. Found: C, 62.20; H, 4.88; N, 16.90.

1-(4-Chloroacetamidophenyl)-4-(cyclohexylmethyl)-1*H*-1,2,3-triazole (*anti*-4d). ^{1}H NMR (400 MHz, CD_3SOCD_3) δ 10.53 (s, 1H, NH), 8.48 (s, 1H, triazole), 7.84 (d, J = 9.0 Hz, 2H, phenyl), 7.77 (d, J = 9.0 Hz, 2H, phenyl), 4.29 (s, 2H, $ClCH_2CO$), 2.57 (d, J = 6.9 Hz, 2H, $ArCH_2$), 1.76 − 1.55 (m, 6H, cyclohexyl-2a/6a, cyclohexyl-3a/5a, cyclohexyl-4a, cyclohexyl-1), 1.28−1.05 (m, 3H, cyclohexyl-3b/5b, cyclohexyl-4b), 1.05 − 0.89 (m, 2H, cyclohexyl-2b/6b). ^{13}C NMR (101 MHz, CD_3SOCD_3) δ 164.88 (C═O), 146.55 (C-Ar), 138.36 (C-Ar), 132.50 (C-Ar), 120.44 (CH-phenyl), 120.36 (CH-triazole), 120.16 (CH-phenyl), 43.53 ($ClCH_2CO$), 37.49 (cyclohexyl-1), 32.70 ($ArCH_2$), 32.47 (cyclohexyl-2/6), 25.94 (cyclohexyl-4), 25.64 (cyclohexyl-3/5). ESI-MS (*m*/*z*, relative intensity): 333 ([M + H]$^+$, 100). Anal. Calcd for $C_{17}H_{21}N_4OCl$: C, 61.35; H, 6.36; N, 16.83. Found: C, 61.09; H, 6.27; N, 16.66.

1-(4-Chloroacetamidophenyl)-4-(naphthalen-2-yl)-1*H*-1,2,3-triazole (*anti*-4e). ^{1}H NMR (400 MHz, CD_3SOCD_3) δ 10.60 (s, 1H, NH), 9.38 (s, 1H, triazole), 8.51 (s, 1H, naphthalene-1), 8.09 (d, J = 8.6 Hz, 1H, naphthalene-3/4), 8.05 (d, J = 8.6 Hz, 1H, naphthalene-4/3), 8.01 (d, J = 7.7 Hz, 1H, naphthalene-5/8), 7.96 (d, J = 8.7 Hz, 3H, phenyl, naphthalene-8/5), 7.85 (d, J = 8.7 Hz, 2H, phenyl), 7.64−7.47 (m, 2H, naphthalene-6/7), 4.32 (s, 2H, $ClCH_2CO$). ^{13}C NMR (101 MHz, CD_3SOCD_3) δ 164.95 (C═O), 147.22 (C-Ar), 138.77 (C-Ar), 133.11 (C-Ar), 132.69 (C-Ar), 132.29 (C-Ar), 128.62 (naphthalene-4/3), 128.00 (naphthalene-5/8), 127.74 (C-Ar), 127.72 (naphthalene-8/5), 126.68 (naphthalene-6/7), 126.27 (naphthalene-7/6), 123.70 (naphthalene-1), 123.65 (naphthalene-3/4), 120.75 (CH-phenyl), 120.26 (CH-phenyl), 119.86 (CH-triazole), 43.54 ($ClCH_2CO$). ESI-MS (*m*/*z*, relative intensity): 363 ([M + H]$^+$, 100), 279 (25), 274 (13). Anal. Calcd for $C_{20}H_{15}N_4OCl$: C, 66.21; H, 4.17; N, 15.44. Found: C, 66.45; H, 4.28; N, 15.25.

1-(4-Chloroacetamidophenyl)-4-([1,1′-biphenyl]-4-yl)-1*H*-1,2,3-triazole (*anti*-4f). ^{1}H NMR (400 MHz, CD_3SOCD_3) δ 10.60 (s, 1H, NH), 9.30 (s, 1H, triazole), 8.04 (d, J = 8.4 Hz, 2H, phenyl), 7.94 (d, J = 9.0 Hz, 2H, phenyl), 7.84 (d, J = 9.1 Hz, 2H, phenyl), 7.82 (d, J = 8.4 Hz, 2H, phenyl), 7.74 (d, J = 7.2 Hz, 2H, phenyl-2″/6″), 7.49 (t, J = 7.6 Hz, 2H, phenyl-3″/5″), 7.39 (t, J = 7.3 Hz, 1H, phenyl-4″), 4.32 (s, 2H, $ClCH_2CO$). ^{13}C NMR (101 MHz, CD_3SOCD_3) δ 164.97 (C═O), 146.90 (C-Ar), 139.79 (C-Ar), 139.52 (C-Ar), 138.78 (C-Ar), 132.29 (C-Ar), 129.37 (C-Ar), 128.99 (CH-phenyl-3″/5″), 127.62 (CH-phenyl-4″), 127.23 (CH-phenyl), 126.56 (CH-phenyl-2″/6″), 125.86 (CH-phenyl), 120.76 (CH-phenyl), 120.25 (CH-phenyl), 119.56 (CH-triazole), 43.56 ($ClCH_2CO$). HRMS (ESI-TOF) *m*/*z*: [M + H]$^+$ calcd for $C_{22}H_{18}N_4OCl$ 389.1169; found 389.1153.

1-(4-Chloroacetamidophenyl)-4-(diphenylhydroxymethyl)-1*H*-1,2,3-triazole (*anti*-4g). ^{1}H NMR (400 MHz, CD_3SOCD_3) δ 10.55 (s, 1H, NH), 8.47 (s, 1H, triazole), 7.90 (d, J = 8.8 Hz, 2H, phenyl), 7.78 (d, J = 8.8 Hz, 2H, phenyl), 7.43 (d, J = 7.5 Hz, 4H, phenyl-2′/6′ × 2), 7.31 (t, J = 7.4 Hz, 4H, phenyl-3′/5′ × 2), 7.24 (t, J = 7.2 Hz, 2H, phenyl-4′ × 2), 6.70 (s, 1H, OH), 4.29 (s, 2H, $ClCH_2CO$). ^{13}C NMR (101 MHz, CD_3SOCD_3) δ 164.90 (C═O), 155.06 (C-Ar), 146.78 (C-Ar), 138.54 (C-Ar), 132.30 (C-Ar), 127.58 (CH-phenyl-3′/5′), 127.05 (CH-phenyl-2′/6′), 126.79 (CH-phenyl-4′), 121.05 (CH-triazole), 120.72 (CH-phenyl), 120.13 (CH-phenyl), 75.83 (C-OH), 43.52 ($ClCH_2CO$). HRMS (ESI-TOF) *m*/*z*: [M + H]$^+$ calcd for $C_{23}H_{20}N_4O_2Cl$ 419.1275; found 419.1269.

1-(4-Chloroacetamidophenyl)-4-(2-(3-chlorophenoxy)-1-hydroxyethyl)-1*H*-1,2,3-triazole (*anti*-4h). ^{1}H NMR (400 MHz, CD_3SOCD_3) δ 10.56 (s, 1H, NH), 8.73 (s, 1H, triazole), 7.89 (d, J = 8.9 Hz, 2H, phenyl), 7.80 (d, J = 8.9 Hz, 2H, phenyl), 7.31 (t, J = 8.2 Hz, 1H, phenyl-5′), 7.07 (t, J = 1.9 Hz, 1H, phenyl-2′), 7.00 (dd, J = 7.9, 1.1 Hz, 1H, phenyl-4′/6′), 6.96 (dd, J = 8.4, 2.0 Hz, 1H, phenyl-6′/4′), 5.90 (d, J = 4.7 Hz, 1H, OH), 5.17−5.08 (m, 1H, CH), 4.33 (dd, J = 10.1, 4.3 Hz, 1H, C*H*H′), 4.30 (s, 2H, $ClCH_2CO$), 4.23 (dd, J = 10.0, 7.0 Hz, 1H, CH*H*′). ^{13}C NMR (101 MHz, CD_3SOCD_3) δ 164.94 (C═O), 159.47 (C-Ar), 149.20 (C-Ar), 138.62 (C-Ar), 133.70 (C-Ar), 132.35 (C-Ar), 130.86 (CH-phenyl-5′), 120.92 (CH-triazole), 120.67 (CH-phenyl, CH-phenyl-4′/6′), 120.21 (CH-phenyl), 114.71 (CH-phenyl-2′), 113.76 (CH-phenyl-6′/4′), 71.72 (CH_2), 64.44 (CH), 43.54 ($ClCH_2CO$). ESI-MS (*m*/*z*, relative intensity): 407 ([M + H]$^+$, 100), 361 (46), 279 (26), 274 (18), 183 (10). Anal. Calcd for $C_{18}H_{16}N_4O_3Cl_2$: C, 53.09; H, 3.96; N, 13.76. Found: C, 52.92; H, 3.80; N, 13.48.

1-(4-Chloroacetamidophenyl)-4-(1-hydroxy-2-methylpropyl)-1*H*-1,2,3-triazole (*anti*-4i). ^{1}H NMR (400 MHz, CD_3SOCD_3) δ 10.54 (s, 1H, NH), 8.54 (s, 1H, triazole), 7.89 (d, J = 8.1 Hz, 2H, phenyl), 7.78 (d, J = 8.1 Hz, 2H, phenyl), 5.32 (d, J = 3.9 Hz, 1H, OH), 4.50 (t, J = 4.6 Hz, 1H, C*H*OH), 4.29 (s, 2H, $ClCH_2CO$), 2.13−1.94 (m, 1H, C*H*$(CH_3)_2$), 0.90 (d, J = 6.3 Hz, 3H, CH_3), 0.86 (d, J = 6.4 Hz, 3H, CH_3). ^{13}C NMR (101 MHz, CD_3SOCD_3) δ 164.89 (C═O), 151.88 (C-Ar), 138.41 (C-Ar), 132.47 (C-Ar), 120.46 (CH-phenyl), 120.17 (CH-phenyl), 120.08 (CH-triazole), 70.73 (CHOH), 43.53 ($ClCH_2CO$), 33.63 (*C*H$(CH_3)_2$), 18.64 (CH_3), 17.71 (CH_3). ESI-MS (*m*/*z*, relative intensity): 331 ([M + Na]$^+$, 8), 309 ([M + H]$^+$, 43), 263 (100). Anal. Calcd for $C_{14}H_{17}N_4O_2Cl$: C, 54.46; H, 5.55; N, 18.15. Found: C, 54.28; H, 5.70; N, 18.06.

1-(4-Chloroacetamidophenyl)-4-(cyclopentylmethyl)-1*H*-1,2,3-triazole (*anti*-4j). ^{1}H NMR (400 MHz, CD_3SOCD_3) δ 10.54 (s, 1H, NH), 8.50 (s, 1H, triazole), 7.85 (d, J = 8.8 Hz, 2H, phenyl), 7.78 (d, J = 8.8 Hz, 2H, phenyl), 4.29 (s, 2H, $ClCH_2CO$), 2.69 (d, J = 7.3 Hz, 2H, $ArCH_2$), 2.25−2.11 (m, 1H, cyclopentyl-1), 1.83−1.67 (m, 2H, cyclopentyl-2a/5a), 1.67−1.56 (m, 2H, cyclopentyl-3a/4a), 1.56−1.42 (m, 2H, cyclopentyl-3b/4b), 1.30−1.14 (m, 2H, cyclopentyl-2b/5b). ^{13}C NMR (101 MHz, CD_3SOCD_3) δ 164.87 (C═O), 147.52 (C-Ar), 138.35 (C-Ar), 132.49 (C-Ar), 120.43 (CH-phenyl), 120.16 (CH-phenyl), 120.08 (CH-triazole), 43.52 ($ClCH_2CO$), 39.35 (cyclopentyl-1), 31.88 (cyclopentyl-2/5), 31.04 ($ArCH_2$), 24.64 (cyclopentyl-3/4). HRMS (ESI-TOF) *m*/*z*: [M + H]$^+$ calcd for $C_{16}H_{20}N_4OCl$ 319.1326; found 319.1333.

1-(4-Chloroacetamidophenyl)-4-(diethoxymethyl)-1*H*-1,2,3-triazole (*anti*-4k). ^{1}H NMR (400 MHz, CD_3SOCD_3) δ 10.55 (s, 1H, NH), 8.70 (s, 1H, triazole), 7.91 (d, J = 8.8 Hz, 2H, phenyl), 7.78 (d, J = 8.7 Hz, 2H, phenyl), 5.74 (s, 1H, CH-acetal), 4.30 (s, 2H, $ClCH_2CO$), 3.71−3.48 (m, 4H, CH_2 × 2), 1.17 (t, J = 7.0 Hz, 6H, CH_3 × 2). ^{13}C NMR (101 MHz, CD_3SOCD_3) δ 164.93 (C═O), 146.95 (C-Ar), 138.67 (C-Ar), 132.23 (C-Ar), 121.05 (CH-triazole), 120.81 (CH-phenyl), 120.11 (CH-phenyl), 96.06 (CH-acetal), 60.82 (CH_2), 43.54 ($ClCH_2CO$), 15.10 (CH_3). HRMS (ESI-TOF) m/z: [M + Na]$^+$ calcd for $C_{15}H_{19}N_4O_3NaCl$ 361.1043; found 361.1031.

1-(4-Chloroacetamidophenyl)-4-(((*tert*-butoxycarbonyl)-amino)methyl)-1*H*-1,2,3-triazole (*anti*-4l). ^{1}H NMR (400 MHz, CD_3SOCD_3) δ 10.55 (s, 1H, ArNH), 8.49 (s, 1H, triazole), 7.86 (d, J = 8.9 Hz, 2H, phenyl), 7.78 (d, J = 8.9 Hz, 2H, phenyl), 7.36 (t, J = 5.2 Hz, 1H, BocNH), 4.29 (s, 2H, $ClCH_2CO$), 4.25 (d, J = 5.5 Hz, 2H,

DOI: 10.1021/acs.jmedchem.6b01237
J. Med. Chem. XXXX, XXX, XXX−XXX

$ArCH_2$), 1.39 (s, 9H, $CH_3 \times 3$). ^{13}C NMR (101 MHz, CD_3SOCD_3) δ 164.91 (C═O), 155.56 (C═O), 146.53 (C-Ar), 138.56 (C-Ar), 132.33 (C-Ar), 120.66 (CH-phenyl, CH-triazole), 120.20 (CH-phenyl), 77.97 ($C(CH_3)_3$), 43.52 ($ClCH_2CO$), 35.58 ($ArCH_2$), 28.21 ($CH_3 \times 3$). HRMS (ESI-TOF) m/z: $[M + H]^+$ calcd for $C_{16}H_{21}N_5O_3Cl$ 366.1333; found 366.1329.

1-(4-Chloroacetamidophenyl)-4-(pyridin-3-ylmethyl)-1*H*-1,2,3-triazole (*anti*-4m). ^1H NMR (400 MHz, CD_3SOCD_3) δ 10.62 (s, 1H, NH), 9.37 (s, 1H, triazole), 9.15 (br. s, 1H, pyridine-2), 8.60 (br s, 1H, pyridine-6), 8.30 (d, J = 7.9 Hz, 1H, pyridine-4), 7.92 (d, J = 8.9 Hz, 2H, phenyl), 7.84 (d, J = 8.9 Hz, 2H, phenyl), 7.55 (br s, 1H, pyridine-5), 4.32 (s, 2H, $ClCH_2CO$). ^{13}C NMR (101 MHz, CD_3SOCD_3) δ 165.01 (C═O), 149.22 (CH-pyridine-6), 146.54 (CH-pyridine-2), 144.46 (C-Ar), 138.95 (C-Ar), 132.54 (CH-pyridine-4), 132.14 (C-Ar), 124.17 (CH-pyridine-5), 120.91 (CH-phenyl), 120.30 (CH-triazole), 120.27 (CH-phenyl), 43.57 ($ClCH_2CO$). HRMS (ESI-TOF) m/z: $[M + H]^+$ calcd for $C_{15}H_{13}N_5OCl$ 314.0809; found 314.0808.

1-(4-Acetamidophenyl)-4-(naphthalen-2-yl)-1*H*-1,2,3-triazole (*anti*-6e). ^1H NMR (400 MHz, CD_3SOCD_3) δ 10.25 (s, 1H, NH), 9.36 (s, 1H, triazole), 8.51 (s, 1H, naphthalene-1), 8.08 (d, J = 8.7 Hz, 1H, naphthalene-3/4), 8.04 (d, J = 8.7 Hz, 1H, naphthalene-4/3), 8.00 (d, J = 7.7 Hz, 1H, naphthalene-5/8), 7.95 (d, J = 7.5 Hz, 1H, naphthalene-8/5), 7.91 (d, J = 8.3 Hz, 2H, phenyl), 7.83 (d, J = 8.5 Hz, 2H, phenyl), 7.65−7.46 (m, 2H, naphthalene-6/7), 2.10 (s, 3H, CH_3CO). ^{13}C NMR (101 MHz, CD_3SOCD_3) δ 168.61 (C═O), 147.16 (C-Ar), 139.67 (C-Ar), 133.12 (C-Ar), 132.67 (C-Ar), 131.62 (C-Ar), 128.60 (naphthalene-4/3), 128.00 (naphthalene-5/8), 127.79 (C-Ar), 127.72 (naphthalene-8/5), 126.68 (naphthalene-6/7), 126.25 (naphthalene-7/6), 123.67 (naphthalene-1, naphthalene-3/4), 120.65 (CH-phenyl), 119.82 (CH-phenyl), 119.70 (CH-triazole), 24.05 (CH_3CO). HRMS (ESI-TOF) m/z: $[M + H]^+$ calcd for $C_{20}H_{17}N_4O$ 329.1402; found 329.1404.

1-(4-Acetamidophenyl)-4-([1,1′-biphenyl]-4-yl)-1*H*-1,2,3-triazole (*anti*-6f). ^1H NMR (400 MHz, CD_3SOCD_3) δ 10.25 (s, 1H, NH), 9.28 (s, 1H, triazole), 8.03 (d, J = 8.0 Hz, 2H, phenyl), 7.89 (d, J = 8.8 Hz, 2H, phenyl), 7.86−7.78 (m, 4H, phenyl), 7.74 (d, J = 7.6 Hz, 2H, phenyl-2″/6″), 7.49 (t, J = 7.6 Hz, 2H, phenyl-3″/5″), 7.39 (t, J = 7.4 Hz, 1H, phenyl-4″), 2.10 (s, 3H, CH_3CO). ^{13}C NMR (101 MHz, CD_3SOCD_3) δ 168.59 (C═O), 146.80 (C-Ar), 139.73 (C-Ar), 139.65 (C-Ar), 139.51 (C-Ar), 131.60 (C-Ar), 129.40 (C-Ar), 128.95 (CH-phenyl-3″/5″), 127.58 (CH-phenyl-4″), 127.19 (CH-phenyl), 126.53 (CH-phenyl-2″/6″), 125.82 (CH-phenyl), 120.64 (CH-phenyl), 119.68 (CH-phenyl), 119.49 (CH-triazole), 24.04(CH_3CO). HRMS (ESI-TOF) m/z: $[M + H]^+$ calcd for $C_{22}H_{19}N_4O$ 355.1559; found 355.1557.

1-(4-Acetamidophenyl)-4-(diphenylhydroxymethyl)-1*H*-1,2,3-triazole (*anti*-6g). ^1H NMR (400 MHz, CD_3SOCD_3) δ 10.20 (s, 1H, NH), 8.45 (s, 1H, triazole), 7.84 (d, J = 9.0 Hz, 2H, phenyl), 7.76 (d, J = 8.6 Hz, 2H, phenyl), 7.43 (d, J = 7.2 Hz, 4H, phenyl-2′/6′ × 2), 7.31 (t, J = 7.5 Hz, 4H, phenyl-3′/5′ × 2), 7.24 (t, J = 7.2 Hz, 2H, phenyl-4′ × 2), 6.71 (s, 1H, OH), 2.08 (s, 3H, CH_3CO). ^{13}C NMR (101 MHz, CD_3SOCD_3) δ 168.60 (C═O), 155.03 (C-Ar), 146.83 (C-Ar), 139.47 (C-Ar), 131.65 (C-Ar), 127.62 (CH-phenyl-3′/5′), 127.08 (CH-phenyl-2′/6′), 126.82 (CH-phenyl-4′), 121.03 (CH-triazole), 120.64 (CH-phenyl), 119.61 (CH-phenyl), 75.86 (C-OH), 24.08(CH_3CO). HRMS (ESI-TOF) m/z: $[M + H]^+$ calcd for $C_{23}H_{21}N_4O_2$ 385.1665; found 385.1666.

General Procedure for Ruthenium-Catalyzed Alkyne−Azide Cycloaddition. To the solution of **3** (105 mg, 0.500 mmol) and alkyne (0.600 mmol, 1.2 equiv) in dioxane (3.6 mL) was added $Cp^*RuCl(PPh_3)_2$ (12.0 mg, 0.0150 mmol, 3.0%). The vial was purged with argon, sealed, and heated at 60 °C until TLC analysis showed complete consumption of the starting material (**3**). The reaction mixture was subsequently diluted with water (20 mL) and extracted with ethyl acetate (3 × 20 mL). The organic layers were combined, washed with brine (10 mL), dried over Na_2SO_4, filtered, and evaporated under reduced pressure. The resulting residue was purified by flash chromatography (ethyl acetate/petrol ether) to yield the desired *syn*-triazole (**4**).

1-(4-Chloroacetamidophenyl)-5-(4-nitrophenyl)-1*H*-1,2,3-triazole (*syn*-4b). ^1H NMR (400 MHz, CD_3SOCD_3) δ 10.60 (s, 1H, NH), 8.31 (s, 1H, triazole), 8.25 (d, J = 8.9 Hz, 2H, phenyl), 7.76 (d, J = 8.8 Hz, 2H, phenyl), 7.57 (d, J = 8.9 Hz, 2H, phenyl), 7.43 (d, J = 8.8 Hz, 2H, phenyl), 4.29 (s, 2H, $ClCH_2CO$). ^{13}C NMR (101 MHz, CD_3SOCD_3) δ 165.06 (C═O), 147.50 (C-Ar), 139.73 (C-Ar), 135.82 (C-Ar), 134.13 (CH-triazole), 132.71 (C-Ar), 131.08 (C-Ar), 129.62 (CH-phenyl), 126.39 (CH-phenyl), 123.92 (CH-phenyl), 119.90 (CH-phenyl), 43.48 ($ClCH_2CO$). HRMS (ESI-TOF) m/z: $[M + H]^+$ calcd for $C_{16}H_{13}N_5O_3Cl$ 358.0707; found 358.0703.

1-(4-Chloroacetamidophenyl)-5-benzyl-1*H*-1,2,3-triazole (*syn*-4c). ^1H NMR (400 MHz, CD_3SOCD_3) δ 10.60 (s, 1H, NH), 7.77 (d, J = 8.8 Hz, 2H, phenyl), 7.58 (s, 1H, triazole), 7.48 (d, J = 8.8 Hz, 2H, phenyl), 7.25 (t, J = 7.2 Hz, 2H, phenyl-3′/5′), 7.20 (t, J = 7.2 Hz, 1H, phenyl-4′), 7.05 (d, J = 7.0 Hz, 2H, phenyl-2′/6′), 4.31 (s, 2H, $ClCH_2CO$), 4.08 (s, 2H, $ArCH_2$). ^{13}C NMR (101 MHz, CD_3SOCD_3) δ 165.05 (C═O), 139.45 (C-Ar), 137.42 (C-Ar), 136.95 (C-Ar), 133.04 (CH-triazole), 131.27 (C-Ar), 128.54 (CH-phenyl-3′/5′), 128.40 (CH-phenyl-2′/6′), 126.69 (CH-phenyl-4′), 125.95 (CH-phenyl), 119.75 (CH-phenyl), 43.55 ($ClCH_2CO$), 28.74 ($ArCH_2$). ESI-MS (m/z, relative intensity): 327 ($[M + H]^+$, 100). Anal. Calcd for $C_{17}H_{15}N_4OCl$: C, 62.48; H, 4.63; N, 17.15. Found: C, 62.53; H, 4.78; N, 16.95.

1-(4-Chloroacetamidophenyl)-5-(cyclohexylmethyl)-1*H*-1,2,3-triazole (*syn*-4d). ^1H NMR (400 MHz, CD_3SOCD_3) δ 10.61 (s, 1H, NH), 7.81 (d, J = 8.6 Hz, 2H, phenyl), 7.70 (s, 1H, triazole), 7.50 (d, J = 8.6 Hz, 2H, phenyl), 4.31 (s, 2H, $ClCH_2CO$), 2.55 (d, J = 7.0 Hz, 2H, $ArCH_2$), 1.63−1.47 (m, 5H, cyclohexyl-3a/5a, cyclohexyl-4a, cyclohexyl-2a/6a), 1.47−1.36 (m,1H, cyclohexyl-1), 1.20−0.97 (m, 3H, cyclohexyl-3b/5b, cyclohexyl-4b), 0.80 (q, J = 11.2 Hz, 2H, cyclohexyl-2b/6b). ^{13}C NMR (101 MHz, CD_3SOCD_3) δ 165.05 (C═O), 139.41 (C-Ar), 136.91 (C-Ar), 132.48 (CH-triazole), 131.47 (C-Ar), 126.18 (CH-phenyl), 119.85 (CH-phenyl), 43.53 ($ClCH_2CO$), 36.56 (cyclohexyl-1), 32.25 (cyclohexyl-2/6), 30.10 ($ArCH_2$), 25.65 (cyclohexyl-4), 25.36 (cyclohexyl-3/5). EI-MS (m/z, relative intensity): 332 (M^+, 41), 250 (30), 221 (100), 91 (50), 77 (55), 65 (40). Anal. Calcd for $C_{17}H_{21}N_4OCl$: C, 61.35; H, 6.36; N, 16.83. Found: C, 61.17; H, 6.45; N, 16.78.

1-(4-Chloroacetamidophenyl)-5-(naphthalen-2-yl)-1*H*-1,2,3-triazole (*syn*-4e). ^1H NMR (400 MHz, CD_3SOCD_3) δ 10.57 (s, 1H, NH), 8.23 (s, 1H, triazole), 7.97 (s, 1H, naphthalene-1), 7.95−7.89 (m, 2H, naphthalene-3/4/5/8), 7.89−7.83 (m, 1H, naphthalene-8/5), 7.73 (d, J = 8.8 Hz, 2H, phenyl), 7.61−7.52 (m, 2H, naphthalene-6/7), 7.43 (d, J = 8.8 Hz, 2H, phenyl), 7.28 (dd, J = 8.5, 1.5 Hz, 1H, naphthalene-4/3), 4.28 (s, 2H, $ClCH_2CO$). ^{13}C NMR (101 MHz, CD_3SOCD_3) δ 164.99 (C═O), 139.41 (C-Ar), 137.58 (C-Ar), 133.29 (CH-triazole), 132.60 (C-Ar), 132.49 (C-Ar), 131.60 (C-Ar), 128.34 (CH-naphthalene), 128.08 (CH-naphthalene), 128.00 (CH-naphthalene), 127.61 (CH-naphthalene), 127.19 (CH-naphthalene-6/7), 126.90 (CH-naphthalene-7/6), 126.26 (CH-phenyl), 125.44 (naphthalene-4/3), 123.73 (C-Ar), 119.81 (CH-phenyl), 43.48 ($ClCH_2CO$). HRMS (ESI-TOF) m/z: $[M + H]^+$ calcd for $C_{20}H_{16}N_4OCl$ 363.1013; found 363.1016.

1-(4-Chloroacetamidophenyl)-5-([1,1′-biphenyl]-4-yl)-1*H*-1,2,3-triazole (*syn*-4f). ^1H NMR (400 MHz, CD_3SOCD_3) δ 10.62 (s, 1H, NH), 8.19 (s, 1H, triazole), 7.77 (d, J = 8.8 Hz, 2H, phenyl), 7.72 (d, J = 8.4 Hz, 2H, phenyl), 7.69 (d, J = 7.3 Hz, 2H, phenyl-2″/6″), 7.52−7.41 (m, 4H, phenyl), 7.41−7.31 (m, 3H, phenyl), 4.30 (s, 2H, $ClCH_2CO$). ^{13}C NMR (101 MHz, CD_3SOCD_3) δ 165.09 (C═O), 140.68 (C-Ar), 139.57 (C-Ar), 138.90 (C-Ar), 137.28 (C-Ar), 133.10 (CH-triazole), 131.68 (C-Ar), 129.02 (CH-phenyl-3″/5″), 128.82 (CH-phenyl), 127.96 (CH-phenyl-4″), 127.02 (CH-phenyl), 126.68 (CH-phenyl-2″/6″), 126.52 (CH-phenyl), 125.27 (C-Ar), 119.88 (CH-phenyl), 43.56 ($ClCH_2CO$). HRMS (EI-TOF) m/z: $[M]^+$ calcd for $C_{22}H_{17}N_4OCl$ 388.1091; found 388.1092.

1-(4-Chloroacetamidophenyl)-5-(diphenylhydroxymethyl)-1*H*-1,2,3-triazole (*syn*-4g). ^1H NMR (400 MHz, CD_3SOCD_3) δ 10.39 (s, 1H, NH), 7.44 (d, J = 8.9 Hz, 2H, phenyl), 7.31−7.18 (m, 10H, phenyl-2′/3′/4′/5′/6′ × 2), 7.15 (s, 1H, triazole), 7.14 (d, J = 8.9 Hz, 2H, phenyl), 6.96 (s, 1H, OH), 4.25 (s, 2H, $ClCH_2CO$). ^{13}C

DOI: 10.1021/acs.jmedchem.6b01237
J. Med. Chem. XXXX, XXX, XXX−XXX

NMR (101 MHz, CD_3SOCD_3) δ 164.82 (C═O), 144.67 (C-Ar), 143.96 (C-Ar), 138.72 (C-Ar), 134.51(CH-triazole), 132.74 (C-Ar), 127.81 (CH-phenyl-2′/6′/3′/5′), 127.32 (CH-phenyl/phenyl-4′), 127.28 (CH-phenyl-4′/phenyl), 126.53 (CH-phenyl-3′/5′/2′/6′), 118.23 (CH-phenyl), 74.75 (C-OH), 43.52 ($ClCH_2CO$). EI-MS (*m*/*z*, relative intensity): 418 (M^+, 3), 236 (42), 208 (82), 182 (87), 131 (94), 105 (100), 91 (51), 77 (100), 63 (64), 51 (85). Anal. Calcd for $C_{23}H_{19}N_4O_2Cl$: C, 65.95; H, 4.57; N, 13.38. Found: C, 66.18; H, 4.67; N, 13.21.

1-(4-Chloroacetamidophenyl)-5-(2-(3-chlorophenoxy)-1-hydroxyethyl)-1*H*-1,2,3-triazole (*syn*-4h). ^1H NMR (400 MHz, CD_3SOCD_3) δ 10.63 (s, 1H, NH), 8.00 (s, 1H, triazole), 7.82 (d, *J* = 8.9 Hz, 2H, phenyl), 7.61 (d, *J* = 8.8 Hz, 2H, phenyl), 7.27 (t, *J* = 8.3 Hz, 1H, phenyl-5′), 7.03−6.94 (m, 2H, phenyl-2′, phenyl-4′/6′), 6.92−6.83 (m, 1H, phenyl-6′/4′), 6.08 (s, 1H, OH), 4.95 (t, *J* = 5.8 Hz, 1H, CH), 4.32 (s, 2H, $ClCH_2CO$), 4.27−4.15 (m, 2H, CH_2). ^{13}C NMR (101 MHz, CD_3SOCD_3) δ 165.09 (C═O), 159.02 (C-Ar), 139.63 (C-Ar), 138.55 (C-Ar), 133.72 (C-Ar), 132.33 (CH-triazole), 131.38 (C-Ar), 130.83(CH-phenyl-5′), 126.08 (CH-phenyl), 120.86 (CH-phenyl-4′/6′), 119.85 (CH-phenyl), 114.59 (CH-phenyl-2′), 113.77 (CH-phenyl-6′/4′), 70.62 (CH_2), 61.56 (CH), 43.56 ($ClCH_2CO$). HRMS (ESI-TOF) *m*/*z*: $[M + H]^+$ calcd for $C_{18}H_{17}N_4O_3Cl_2$ 407.0678; found 407.0677.

1-(4-Chloroacetamidophenyl)-5-(1-hydroxy-2-methylpropyl)-1*H*-1,2,3-triazole (*syn*-4i). ^1H NMR (400 MHz, CD_3SOCD_3) δ 10.63 (s, 1H, NH), 7.81 (d, *J* = 8.7 Hz, 2H, phenyl), 7.80 (s, 1H, triazole), 7.54 (d, *J* = 8.8 Hz, 2H, phenyl), 5.62 (d, *J* = 5.5 Hz, 1H, OH), 4.32 (s, 2H, $ClCH_2CO$), 4.26 (dd, *J* = 7.4, 5.5 Hz, 1H, C*H*OH), 1.91−1.75 (m, 1H, $CH(CH_3)_2$), 0.83 (d, *J* = 6.6 Hz, 3H, CH_3), 0.65 (d, *J* = 6.7 Hz, 3H, CH_3). ^{13}C NMR (101 MHz, CD_3SOCD_3) δ 165.10 (C═O), 141.13 (C-Ar), 139.52 (C-Ar), 131.87 (CH-triazole), 131.66 (C-Ar), 126.29 (CH-phenyl), 119.84 (CH-phenyl), 68.25 (CHOH), 43.57 ($ClCH_2CO$), 33.15 ($CH(CH_3)_2$), 18.83 (CH_3), 18.06 (CH_3). ESI-MS (*m*/*z*, relative intensity): 309 ($[M + H]^+$, 100). Anal. Calcd for $C_{14}H_{17}N_4O_2Cl$: C, 54.46; H, 5.55; N, 18.15. Found: C, 54.50; H, 5.60; N, 18.03.

1-(4-Chloroacetamidophenyl)-5-(diethoxymethyl)-1*H*-1,2,3-triazole (*syn*-4k). ^1H NMR (400 MHz, CD_3SOCD_3) δ 10.61 (s, 1H, NH), 7.85 (s, 1H, triazole), 7.79 (d, *J* = 8.9 Hz, 2H, phenyl), 7.58 (d, *J* = 8.9 Hz, 2H, phenyl), 5.79 (s, 1H, CH-acetal), 4.32 (s, 2H, $ClCH_2CO$), 3.55−3.38 (m, 4H, $CH_2 \times 2$), 1.02 (t, *J* = 7.0 Hz, 6H, $CH_3 \times 2$). ^{13}C NMR (101 MHz, CD_3SOCD_3) δ 165.05 (C═O), 139.47 (C-Ar), 136.30 (C-Ar), 132.90 (CH-triazole), 131.72 (C-Ar), 125.68 (CH-phenyl), 119.58 (CH-phenyl), 94.28 (CH-acetal), 61.37 (CH_2), 43.56 ($ClCH_2CO$), 14.86 (CH_3). ESI-MS (*m*/*z*, relative intensity): 339 ($[M + H]^+$, 100), 237 (14). Anal. Calcd for $C_{15}H_{19}N_4O_3Cl$: C, 53.18; H, 5.65; N, 16.54. Found: C, 53.42; H, 5.68; N, 16.30.

■ ASSOCIATED CONTENT

Supporting Information

The Supporting Information is available free of charge on the ACS Publications website at DOI: 10.1021/acs.jmedchem.6b01237.

Additional figures, NMR spectra, and HCD fragmentation of peptides (PDF)

■ AUTHOR INFORMATION

Corresponding Author

*E-mail: yuewang@ucas.ac.cn; yuewang@bjmu.edu.cn. Phone: +86-10-88256092. Fax: +86-10-88256092.

ORCID

Yue Wang: 0000-0002-2574-6306

Notes

The authors declare no competing financial interest.

■ ACKNOWLEDGMENTS

This work was financially supported by the National Natural Science Foundation of China (Grant 21302182), China Postdoctoral Science Foundation (Grants 2013M540133, 2014T70113), and the State Key Laboratory of Natural and Biomimetic Drugs (Grants K20130211, K20140210, K20150207). We thank the Protein Chemistry Facility at the Center for Biomedical Analysis of Tsinghua University for sample analysis.

■ ABBREVIATIONS USED

APBT, 1-(4-acetamidophenyl)-4-([1,1′-biphenyl]-4-yl)-1*H*-1,2,3-triazole; APNT, 1-(4-acetamidophenyl)-4-(naphthalen-2-yl)-1*H*-1,2,3-triazole; BADGP, benzyl-2-acetamido-2-deoxy-α-D-galactopyranoside; BZX, benzoxazolinone; Con A, concanavalin A; CuAAC, copper-catalyzed azide−alkyne cycloaddition; DBA, *Dolichos biflorus*; DMEM, Dulbecco's modified Eagle medium; ECL, *Erythrina cristagalli*; GSL-I, *Griffonia* (*Bandeiraea*) *simplicifolia* I; HCD, higher energy collisional dissociation; HRP, horseradish peroxidase; LCA, *Lens culinaris*; OGA, *O*-GlcNAcase; OGT, *O*-GlcNAc transferase; PHA-E, *Phaseolus vulgaris* erythroagglutinin; PNA, peanut agglutinin; PUGNAc, (*Z*)-*O*-(2-acetamido-2-deoxy-D-glucopyranosylidene)amino *N*-phenylcarbamate; PVDF, polyvinylidene fluoride; RuAAC, ruthenium-catalyzed azide−alkyne cycloaddition; TGS, target-guided synthesis; TISCC, tethering in situ click chemistry

■ REFERENCES

(1) Torres, C. R.; Hart, G. W. Topography and polypeptide distribution of terminal *N*-acetylglucosamine residues on the surfaces of intact lymphocytes. Evidence for *O*-linked GlcNAc. *J. Biol. Chem.* **1984**, *259*, 3308−3317.

(2) Haltiwanger, R. S.; Holt, G. D.; Hart, G. W. Enzymatic addition of *O*-GlcNAc to nuclear and cytoplasmic proteins. Identification of a uridine diphospho-*N*-acetylglucosamine:peptide β-*N*-acetylglucosaminyltransferase. *J. Biol. Chem.* **1990**, *265*, 2563−2568.

(3) Gambetta, M. C.; Müller, J. A critical perspective of the diverse roles of *O*-GlcNAc transferase in chromatin. *Chromosoma* **2015**, *124*, 429−442.

(4) Dias, W. B.; Cheung, W. D.; Wang, Z. H.; Hart, G. W. Regulation of calcium/calmodulin-dependent kinase IV by *O*-GlcNAc modification. *J. Biol. Chem.* **2009**, *284*, 21327−21337.

(5) Hart, G. W.; Housley, M. P.; Slawson, C. Cycling of *O*-linked β-*N*-acetylglucosamine on nucleocytoplasmic proteins. *Nature* **2007**, *446*, 1017−1022.

(6) Fujiki, R.; Chikanishi, T.; Hashiba, W.; Ito, H.; Takada, I.; Roeder, R. G.; Kitagawa, H.; Kato, S. GlcNAcylation of a histone methyltransferase in retinoic-acid-induced granulopoiesis. *Nature* **2009**, *459*, 455−459.

(7) Yang, X. Y.; Ongusaha, P. P.; Miles, P. D.; Havstad, J. C.; Zhang, F. X.; So, W. V.; Kudlow, J. E.; Michell, R. H.; Olefsky, J. M.; Field, S. J.; Evans, R. M. Phosphoinositide signalling links *O*-GlcNAc transferase to insulin resistance. *Nature* **2008**, *451*, 964−U1.

(8) Vaidyanathan, K.; Wells, L. Multiple tissue-specific roles for the *O*-GlcNAc post-translational modification in the induction of and complications arising from type II diabetes. *J. Biol. Chem.* **2014**, *289*, 34466−34471.

(9) Singh, J. P.; Zhang, K.; Wu, J.; Yang, X. *O*-GlcNAc signaling in cancer metabolism and epigenetics. *Cancer Lett.* **2015**, *356*, 244−250.

(10) Marsh, S. A.; Collins, H. E.; Chatham, J. C. Protein *O*-GlcNAcylation and cardiovascular (patho)physiology. *J. Biol. Chem.* **2014**, *289*, 34449−34456.

(11) Yuzwa, S. A.; Vocadlo, D. J. *O*-GlcNAc and neurodegeneration: biochemical mechanisms and potential roles in Alzheimer's disease and beyond. *Chem. Soc. Rev.* **2014**, *43*, 6839−6858.

DOI: 10.1021/acs.jmedchem.6b01237
J. Med. Chem. XXXX, XXX, XXX−XXX

(12) Wang, Y. *O*-GlcNAc transferase and its inhibitors. *Huaxue Xuebao* **2013**, *71*, 1477−1487.
(13) Konrad, R. J.; Zhang, F.; Hale, J. E.; Knierman, M. D.; Becker, G. W.; Kudlow, J. E. Alloxan is an inhibitor of the enzyme *O*-linked *N*-acetylglucosamine transferase. *Biochem. Biophys. Res. Commun.* **2002**, *293*, 207−212.
(14) Kang, E.-S.; Han, D.; Park, J.; Kwak, T. K.; Oh, M.-A.; Lee, S.-A.; Choi, S.; Park, Z. Y.; Kim, Y.; Lee, J. W. *O*-GlcNAc modulation at Akt1 Ser473 correlates with apoptosis of murine pancreatic β cells. *Exp. Cell Res.* **2008**, *314*, 2238−2248.
(15) Gloster, T. M.; Zandberg, W. F.; Heinonen, J. E.; Shen, D. L.; Deng, L. H.; Vocadlo, D. J. Hijacking a biosynthetic pathway yields a glycosyltransferase inhibitor within cells. *Nat. Chem. Biol.* **2011**, *7*, 174−181.
(16) Jiang, J. Y.; Lazarus, M. B.; Pasquina, L.; Sliz, P.; Walker, S. A neutral diphosphate mimic crosslinks the active site of human *O*-GlcNAc transferase. *Nat. Chem. Biol.* **2012**, *8*, 72−77.
(17) Ortiz-Meoz, R. F.; Jiang, J.; Lazarus, M. B.; Orman, M.; Janetzko, J.; Fan, C.; Duveau, D. Y.; Tan, Z.-W.; Thomas, C. J.; Walker, S. A small molecule that inhibits OGT activity in cells. *ACS Chem. Biol.* **2015**, *10*, 1392−1397.
(18) Lee, T. N.; Alborn, W. E.; Knierman, M. D.; Konrad, R. J. Alloxan is an inhibitor of *O*-GlcNAc-selective *N*-acetyl-β-D-glucosaminidase. *Biochem. Biophys. Res. Commun.* **2006**, *350*, 1038−1043.
(19) Hennebicq-Reig, S.; Lesuffleur, T.; Capon, C.; Bolos, C. d.; Kim, I.; Moreau, O.; Richet, C.; HÉMon, B.; Recchi, M.-A.; Maës, E.; Aubert, J.-P.; Real, F. X.; Zweibaum, A.; Delannoy, P.; Degand, P.; Huet, G. Permanent exposure of mucin-secreting HT-29 cells to benzyl-*N*-acetyl-α-D-galactosaminide induces abnormal *O*-glycosylation of mucins and inhibits constitutive and stimulated MUC5AC secretion. *Biochem. J.* **1998**, *334*, 283−295.
(20) Erlanson, D. A.; Braisted, A. C.; Raphael, D. R.; Randal, M.; Stroud, R. M.; Gordon, E. M.; Wells, J. A. Site-directed ligand discovery. *Proc. Natl. Acad. Sci. U. S. A.* **2000**, *97*, 9367−9372.
(21) Erlanson, D. A.; Wells, J. A.; Braisted, A. C. Tethering: Fragment-based drug discovery. *Annu. Rev. Biophys. Biomol. Struct.* **2004**, *33*, 199−223.
(22) Lewis, W. G.; Green, L. G.; Grynszpan, F.; Radić, Z.; Carlier, P. R.; Taylor, P.; Finn, M. G.; Sharpless, K. B. Click chemistry in situ: Acetylcholinesterase as a reaction vessel for the selective assembly of a femtomolar inhibitor from an array of building blocks. *Angew. Chem., Int. Ed.* **2002**, *41*, 1053−1057.
(23) Sharpless, K. B.; Manetsch, R. In situ click chemistry: A powerful means for lead discovery. *Expert Opin. Drug Discovery* **2006**, *1*, 525−538.
(24) Mamidyala, S. K.; Finn, M. G. In situ click chemistry: Probing the binding landscapes of biological molecules. *Chem. Soc. Rev.* **2010**, *39*, 1252−1261.
(25) Lundell, N.; Schreitmüller, T. Sample preparation for peptide mapping — A pharmaceutical quality-control perspective. *Anal. Biochem.* **1999**, *266*, 31−47.
(26) Smythe, C. V. The reaction of iodoacetate and of iodoacetamide with various sulfhydryl groups, with urease, and with yeast preparations. *J. Biol. Chem.* **1936**, *114*, 601−612.
(27) Anson, M. L. The reactions of iodine and iodoacetamide with native egg albumin. *J. Gen. Physiol.* **1940**, *23*, 321−331.
(28) Zhang, J. D.; Lee, M. H.; Walker, G. C. *p*-Azidoiodoacetanilide, a new short photocrosslinker that has greater cysteine specificity than *p*-azidophenacyl bromide and *p*-azidobromoacetanilide. *Biochem. Biophys. Res. Commun.* **1995**, *217*, 1177−1184.
(29) Grimster, N. P.; Stump, B.; Fotsing, J. R.; Weide, T.; Talley, T. T.; Yamauchi, J. G.; Nemecz, Á.; Kim, C.; Ho, K.-Y.; Sharpless, K. B.; Taylor, P.; Fokin, V. V. Generation of candidate ligands for nicotinic acetylcholine receptors via in situ click chemistry with a soluble acetylcholine binding protein template. *J. Am. Chem. Soc.* **2012**, *134*, 6732−6740.
(30) Yamauchi, J. G.; Gomez, K.; Grimster, N.; Dufouil, M.; Nemecz, Á.; Fotsing, J. R.; Ho, K.-Y.; Talley, T. T.; Sharpless, K. B.; Fokin, V. V.; Taylor, P. Synthesis of selective agonists for the α7 nicotinic acetylcholine receptor with in situ click-chemistry on acetylcholine-binding protein templates. *Mol. Pharmacol.* **2012**, *82*, 687−699.
(31) Compounds ***syn*-4a** and ***syn*-4j** were difficult to purify and had to be abandoned.
(32) Xu, Y.; Pang, W.; Lu, J.; Shan, A.; Zhang, Y. Polypeptide *N*-acetylgalactosaminyltransferase 13 contributes to neurogenesis via stabilizing the mucin-type *O*-glycoprotein podoplanin. *J. Biol. Chem.* **2016**, *291*, 23477−23488.
(33) Whiting, M.; Muldoon, J.; Lin, Y.-C.; Silverman, S. M.; Lindstrom, W.; Olson, A. J.; Kolb, H. C.; Finn, M. G.; Sharpless, K. B.; Elder, J. H.; Fokin, V. V. Inhibitors of HIV-1 protease by using in situ click chemistry. *Angew. Chem., Int. Ed.* **2006**, *45*, 1435−1439.
(34) Hirose, T.; Sunazuka, T.; Sugawara, A.; Endo, A.; Iguchi, K.; Yamamoto, T.; Ui, H.; Shiomi, K.; Watanabe, T.; Sharpless, K. B.; Omura, S. Chitinase inhibitors: Extraction of the active framework from natural argifin and use of in situ click chemistry. *J. Antibiot.* **2009**, *62*, 277−282.
(35) Tieu, W.; Soares da Costa, T. P.; Yap, M. Y.; Keeling, K. L.; Wilce, M. C. J.; Wallace, J. C.; Booker, G. W.; Polyak, S. W.; Abell, A. D. Optimising in situ click chemistry: The screening and identification of biotin protein ligase inhibitors. *Chem. Sci.* **2013**, *4*, 3533−3537.
(36) Lee, L. V.; Mitchell, M. L.; Huang, S.-J.; Fokin, V. V.; Sharpless, K. B.; Wong, C.-H. A potent and highly selective inhibitor of human α-1,3-fucosyltransferase via click chemistry. *J. Am. Chem. Soc.* **2003**, *125*, 9588−9589.
(37) Das, S.; Pati, D.; Tiwari, N.; Nisal, A.; Sen Gupta, S. Synthesis of silk fibroin-glycopolypeptide conjugates and their recognition with lectin. *Biomacromolecules* **2012**, *13*, 3695−3702.

DOI: 10.1021/acs.jmedchem.6b01237
J. Med. Chem. XXXX, XXX, XXX−XXX